Jurnal Rekayasa Kimia dan Lingkungan
(Journal of Chemical Engineering and Environment)
Vol. 19, No. 2, Page 237 - 250, December 2024
ISSN 1412-5064, e-ISSN 2356-1661
https://doi.org/10.23955/rkl.v19i2.41399

# Study on Carbon Dioxide ($CO_2$) Adsorption Using Chemically Activated Serpentine as an Adsorbent

**Muhammad Fannka Dhedia[1], Mahidin[2,*], Husni Husin[2], Hisbullah[2], Nasrullah Razali[2], A. A. Reza[3] and Abdul Hadi[4]**

[1]Master Program, Department of Chemical Engineering, Universitas Syiah Kuala, Kopelma Darussalam, 23111, Banda Aceh, Indonesia
[2]Department of Chemical Engineering, Universitas Syiah Kuala, Kopelma Darussalam, 23111, Banda Aceh, Indonesia
[3]Doctoral Program of Engineering Studies, Universitas Syiah Kuala, Kopelam, Darussalam, 23111, Banda Aceh, Indonesia
[4]Center for Chemical Engineering Studies, Universiti Teknologi MARA Cawangan Pulau Pinang, 13500 Permatang Pauh, Pulau Pinang, Malaysia
*E-mail: mahidin@usk.ac.id

Article History
Received: 27 September 2024; Received in Revision: 4 November 2024; Accepted: 29 November 2024

**Abstract**

The increase in carbon emissions resulting from industrial activities has become a major concern for environmental and climate conditions. Carbon Capture and Storage (CCS) represents a significant effort to mitigate the $CO_2$ problem. Aceh Province possesses a potential distribution of serpentine, which may serve as an effective material for CCS applications. This study evaluates the effects of gas flow rate, particle size, sorbent weight, and pressure on $CO_2$ adsorption using chemically activated serpentine. The activation process involved hydrochloric acid (HCl) at three concentrations: 8%, 9%, and 10%, with particle sizes of 50 mesh, 100 mesh, and 150 mesh. Activation was conducted at room temperature with an acid-to-serpentine ratio of 10:1 for 30 minutes. Adsorption tests were performed at ambient temperature under pressures of 2, 3, and 4 bar, with adsorption times of 30, 60, and 120 minutes. Results indicate that activated serpentine treated with 9% HCl and a particle size of 150 mesh achieved the highest performance, demonstrating an adsorption efficiency of 33.01% and an adsorption capacity of 82.22% (0.0488 g $CO_2$/g adsorbent) at a pressure of 2 bar. Both the Langmuir and Freundlich isotherm models closely fit the data ($R^2 = 1$). This study concludes that HCl activation significantly enhances the capacity and efficiency of serpentine as a $CO_2$ adsorbent.

Keywords: serpentine, chemical activation, HCl, $CO_2$, carbon capture and storage.



## 1. Introduction

The increase in atmospheric carbon dioxide ($CO_2$) levels has become a major environmental challenge, leading to a global push for carbon neutrality by 2030. This ambition is supported by the 2015 Paris Agreement, which aims to limit global temperature rise to below 2°C (Burke and Fishel, 2020). However, current efforts to reduce greenhouse gas emissions are insufficient to meet this target. Developing regions, such as parts of Asia, face unique challenges in transitioning away from coal due to infrastructure limitations and high costs as reported by Russel, (2023), making Carbon Capture and Storage (CCS) technologies particularly vital in these areas.

Aceh Province in Indonesia shows potential in contributing to carbon mitigation efforts using locally abundant serpentine rock as an adsorbent for $CO_2$. The unique mineral composition of serpentine, rich in magnesium and other minerals, offers a promising material for $CO_2$ adsorption, as it can be chemically activated to enhance its adsorption capacity (Ardiansyah et al., 2019). However, the usage of serpentine in $CO_2$ capture remains underexplored, particularly in its raw or minimally processed forms.

On the previous work, the usage of the serpentine as the adsorbent for $CO_2$ is commonly found in the hydrothermal or thermal method for its activation. The method for activation for the serpentine limited when it comes to the chemical activation. For



**To cite this article:** Dhedia, M. F., Mahidin, H., Husin, H., Hisbullah, N. R., Reza, A. A., Hadi, A. (2024). Study on Carbon Dioxide (CO2) Adsorption Using Chemically Activated Serpentine as an Adsorbent. *Jurnal Rekayasa Kimia & Lingkungan* 19 (2): 237 - 250. https://doi.org/10.23955/rkl.v19i2. 41399

example, the work that has done by Sanna (2017) that share the similar method which involving chemical process where they're using the serpentine to adsorb $CO_2$ using the $NaHSO_4$ by leaching the serpentine and the carbonation process is captured in the form of $Na_2CO_3$. They are achieving the results at 69.6% of dissolution efficiency using the 100°C and carbonation efficiency is at 95.4% at 90°C with 1:1 magnesium to sodium carbonate molar ratio. Another method which involving chemistry activation is Lin (2008) where the usage of NaOH is required to increase the pH for the serpentine precipitation process right after using the HCl which gives the result of the $CO_2$ adsorption 4.4 mmol/g for serpentine derived and its $Mg(OH)_2$ reagent grade at the value 1.6 mmol/g.

Solid adsorbents like activated carbon, and zeolites have shown considerable promise for $CO_2$ capture due to their high adsorption efficiency, reusability, and cost-effectiveness. Research conducted by Kim and Kim (2023), where they compared $CO_2$ adsorption performance across these materials, finding that zeolites have the highest $CO_2$ uptake at low pressures due to their surface heterogeneity. Activated carbon and specific metal-organic frameworks (MOFs) like MSP, however, exhibit stronger performance at higher pressures, where larger pore volume and surface area significantly increase $CO_2$ uptake capacity with working capacity 25°C ranged from 0.78 to 6.50 mmol/g.

On the contrary, chemical activation using acids, particularly hydrochloric acid (HCl), presents a simpler and more energy efficient approach. Yet, this method has not yet been applied to serpentine, especially the serpentine reserves in Aceh, which are uniquely positioned for CCS applications for its abundance and mineral composition. This study investigates the chemically activated serpentine which highlights the significant research gap.

This study aims to evaluate the effect of various operational parameters, including gas flow rate, serpentine particle size, sorbent weight, and pressure, on $CO_2$ adsorption efficiency using chemically activated serpentine from Aceh. This research will focus on optimizing these parameters to maximize the adsorption capacity and efficiency of serpentine, thereby contributing to the development of more effective CCS technologies.

**Figure 1**. $CO_2$ Adsorption Setup

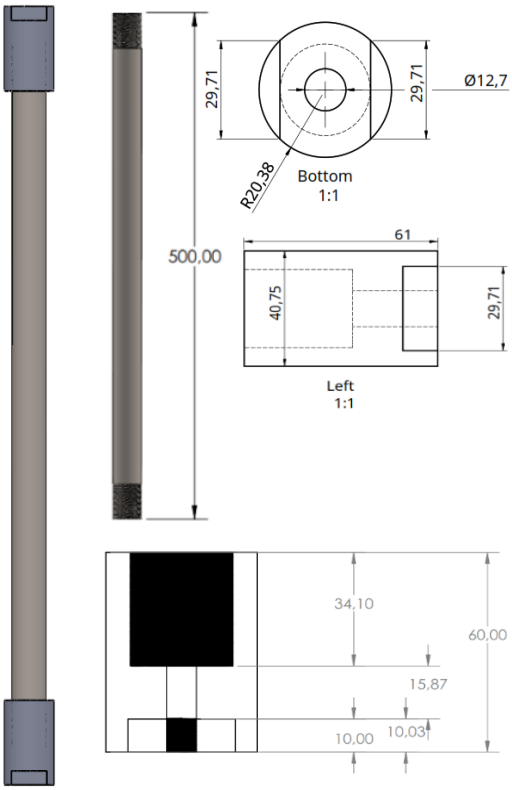


**Figure 2.** Custom-Designed Fluidized Bed Reactor

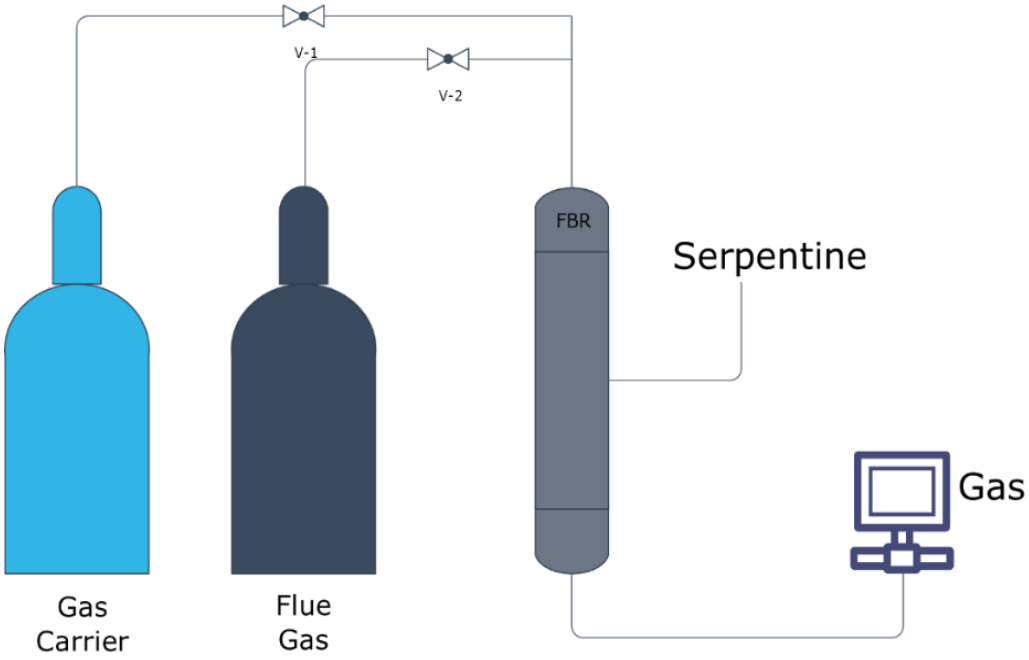


**Figure 3.** Adsorption Schematics

## 2. Methodology

### 2.1. Research Material

The material that we are using is the serpentine taken from Lam Ara Tunong, Kuta Malaka, Cot Glie Aceh Besar, with the NaOH (NaOH Merck), HCl (Hydrochloric Acid, Merck), and $CO_2$ gas.

### 2.2. Serpentine Adsorbent Production

The serpentine samples were sieved to achieve particle sizes of 50 mesh, 100 mesh, and 150 mesh by Sieve Shaker. Activation was performed using HCl solutions at concentrations of 8%, 9%, and 10% (Beglaryan et al., 2023), with a liquid-to-solid volume ratio of 10:1.

Activation was conducted at room temperature for 30 minutes, followed by adjustment of the pH to a range of 8–11 using NaOH (Merck) as described by Lin (2008). The activated samples were then filtered to separate solids and liquids and dried at 100°C for 3 hours using a Memmert UN30 oven dryer.

Once dried, the activated serpentine was introduced into a self-custom-designed fixed bed reactor with the following specifications: Reactor height: 500 mm; Tube internal diameter: 20.10 mm; external diameter: 27.65 mm; Inlet and outlet piping diameter: 12.7 mm.

The reactor was filled with the serpentine adsorbent, sealed with cotton at the inlet, and connected to a $CO_2$ gas source. The $CO_2$ gas was introduced and controlled using a valve installed on the gas tank. Nitrogen was used as a carrier gas and mixed with $CO_2$ before entering the reactor. After the adsorption process, gas analysis was performed using a HORIBA gas analyzer, which was connected to the outlet of the reactor.

For adsorption tests, the $CO_2$ pressures applied were 2 bar, 3 bar, and 4 bar, and the adsorption durations were set to 30 minutes, 60 minutes, and 120 minutes (Tian et al., 2022; Yue et al., 2006). The weight of the adsorbent used in these experiments was 30 grams, with variations applied as required for analysis. The adsorption performance was assessed by measuring the change in $CO_2$ concentration before and after the reaction.

### 2.4. Data Analysis

To understand the performance through the data analysis, we need to calculate the serpentine volume ($V_{serpentine}$) and its reactor volume ($V_{tube}$) with given equation:

$$V_{serpentine} = \frac{m_{serpentine}}{\rho_{serpentine}} \quad (1)$$

$$V_{tube} = \pi \times r^2 \times H \quad (2)$$

$$\text{Gas volume} = V_{tube} - V_{serpentine} \quad (3)$$

remark:
$m_{serpentine}$ = mass of serpentine (g)
$\rho_{serpentine}$ = density of serpentine (g/cm$^3$)
r = radius of the circle (cm)
H = height (cm)

To calculate the results of the obtained data, the equation of the adsorption capacity and the adsorbent efficiency with the equation given below:

$$\%E = \left(\frac{C_o - C_e}{C_o}\right) \times 100\% \quad (4)$$

$$Qe = \left(\frac{C_o - C_e}{m}\right) \times V \quad (5)$$

remark:
%E = adsorption efficiency
$C_o$ = initial weight of the gas (gr $CO_2$)
$C_e$ = final weight of the gas (gr $CO_2$)
Qe = adsorption capacity per molecular weight (gr $CO_2$/gr adsorbent ×10-3)
V = volume of gas (mL)
m = mass of adsorbent (g)

Adsorption isotherms are the adsorption process that takes place at a constant temperature. The adsorption isothermal model used in adsorption is the Langmuir isothermal model (Eq. 6) and the Freundlich isothermal model (Eq. 7) which for these two models are used by Li and Hitch, (2015)

$$q = q_{max} \times K_L \left(\frac{C_e}{1 + K_L \times C_e}\right) \quad (6)$$

$$qe = K_f \times Ce^{\frac{1}{n}} \quad (7)$$

remark:
qe = number of substances adsorbed per gram of adsorbent (mg/g)
Ce = concentration of solute in solution after equilibrium
$K_L$ = constant adsorption Langmuir (L/mg)
$K_f$ and n = adsorption capacity and adsorption intensity
Qmax = maximum adsorption capacity (mg/g)

## 3. Results and Discussion

### 3.1. Characterization Results

#### 3.1.1. XRD Results as the Effect of Acid Concentration

The results showed through Figure 4 is that chemical activation with HCl at higher concentrations significantly affected the decay of the chrysotile structure, resulting in the formation of new secondary phases detected through XRD patterns (Daval et al., 2013; Falini et al., 2004; Vieira et al., 2022a).
In raw serpentine without chemical treatment, XRD shows that chrysotile is the dominant phase with a content of 64.4%. The characteristic peaks of chrysotile appear at 2θ angles of 12.04° and 24.34° with peak intensities of 624.26 counts and 432.22 counts, respectively (Falini et al., 2004). After treatment with 8% HCl, the chrysotile content decreased dramatically to 34.1%, with peak intensities reduced to 194.99 counts at 12.04° and 149.79 counts at 24.34°. This decrease shows that HCl is able to decompose the chrysotile structure significantly (Daval et al., 2013).

Treatment with 8% HCl also causes the formation of new phases such as vesuvianite with a content of 43.0%, which has new peaks at 2θ angles of 10.86°, 19.38°, 21.90°, 24.29°, 34.65°, and 35.47°. The lizardite-1T phase was detected at 8.1%, with a new peak at 12.02° 2θ (Lacinska et al., 2016).

When the HCl concentration was increased to 9%, the chrysotile content decreased further to 32.2%. New phases formed include antigorite-T at 39.8%, $H_8$ $Mg_2$ $Ni_4$ O18 Si4 at 12.2%, and lizardite-2H1 at 4.7% (Li et al., 2023).

In the treatment with 10% HCl, the chrysotile content decreased dramatically to 30.9%, with peak intensities reduced to 1000 counts at 12.15° 2θ and 769.36 counts at 24.43° 2θ. New phases formed at this concentration include antigorite-T at 14.0%, lizardite-2H1 at 13.3%, and sepiolite at 9.5% (Beglaryan et al., 2023).

HCl treatment causes leaching of $Mg^{2+}$ cations from the octahedral layer in the serpentine structure, which plays an important role in the formation of secondary phases. Increasing the HCl concentration from 8% to 10% indicates intensified structural changes, as evidenced by the increased intensity and number of new phases detected by XRD (Vieira, 2022). Treatment with NaOH after activation with HCl removed the remaining cristobalite peaks and indicated the formation of the Mg-oxalate phase. Strong alkaline conditions help convert the secondary Mg-silicate into more stable Mg-hydroxide and Mg-carbonate phases, which are relevant for $CO_2$ sequestration applications (Beglaryan et al., 2023; Lin et al., 2008).
Activation of serpentine with HCl at various concentrations affects the mineral characteristics significantly, mainly through chrysotile decay and the formation of more reactive secondary phases. Increasing HCl

concentration showed a trend towards decreased chrysotile content and increased secondary phase formation, all of which were detected in depth by XRD, providing important insights for the development of serpentine materials in industrial applications such as $CO_2$ sequestration (Daval et al., 2013; Vieira et al., 2022b).

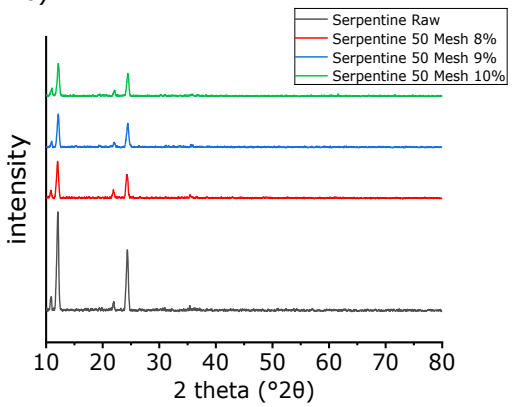


**Figure 4.** XRD Pattern as the Effect of HCl Concentration

### 3.1.2. XRD Results as the Effect of Particle Size

The analytical results show through Figure 5 that smaller particle sizes (with higher mesh counts) significantly increase the surface area available for chemical reactions, which in turn accelerates the decay of chrysotile and the formation of new, more reactive secondary phases (Beglaryan et al., 2023; Lacinska et al., 2016).

In serpentine samples with a particle size of 50 mesh, the chrysotile content decreased from 64.4% in raw serpentine to 34.1% after treatment with 8% HCl. Secondary phases formed from this dissolution process included vesuvianite (43.0%), lizardite-1T (8.1%), lemoynite (6.4%), tschernichite (4.4%), and lazurite (3.9%) (Daval, 2013).

When the particle size was increased to 100 mesh, the chrysotile content further decreased to 25.1% after treatment with 8% HCl. At this size, a wider variety of secondary phases formed, including antigorite-T (17.6%), lizardite (17.4%), percovaite (10.7%), 9-1-4 (7.0%), and lizardite-2H1 (6.8%) (Vieira, 2022).

The finest particle size tested, 150 mesh, showed the most extensive dissolution of chrysotile, with only 14.1% remaining after treatment with 8% HCl. At this size, the most numerous and diverse secondary phases were formed, including antigorite-T (16.9%), $H_8$ $Mg_3$ $Ni_3$ $O_{18}$ Si4 (13.4%), $C_{20}$ $H_{52}$ $Mg_2$ $N_8$ (13.0%), tschernichite (11.4%), $H_6$ Mg $O_6$ Si (11.1%), lizardite-1T (7.0%), and nepouite (4.4%) (Lacinska et al., 2016).

This study shows that the smaller the serpentine particle size, the greater the surface area available for chemical reactions, which increases the efficiency of chrysotile dissolution and accelerates the formation of secondary phases. HCl treatment of smaller particle sizes indicates that the crystal structure of chrysotile is more easily degraded, allowing the formation of new, more stable and reactive phases, which are important for $CO_2$ sequestration applications (Daval et al., 2013; Lacinska et al., 2016; Vieira et al., 2022b).

Follow-up treatment with NaOH after activation with HCl shows that the remaining cristobalite structure can be completely broken down, and the secondary Mg-silicate phase formed can be converted into stable Mg-hydroxide and Mg-carbonate phases. This indicates that a combination of acid and base treatment can be effectively used to improve the adsorption characteristics of serpentine, which is relevant for applications in carbon capture and storage (Beglaryan et al., 2023; Lin et al., 2008).

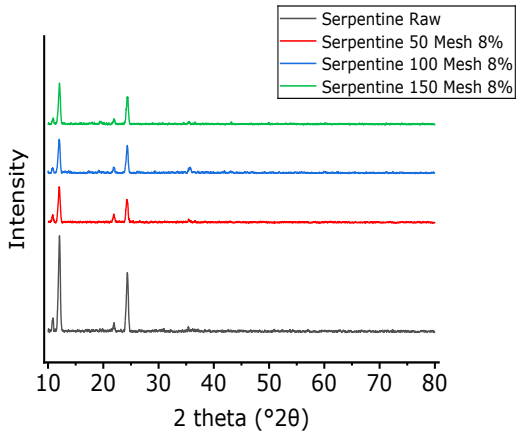


**Figure 5.** XRD Pattern as the Effect of Particle Size

### 3.2. Adsorption Performance Analysis

This test evaluates the ability of serpentine as an adsorbent to capture $CO_2$ in a Fixed Bed Reactor (FBR). The Study employs the single step-by step variables knockout method by Muslim (2022), which systematically eliminates variables that yield suboptimal results based on initial trials. Adsorption efficiency and capacity are calculated by determining the serpentine volume, reactor volume, and gas volume using Equation 1-3. Then proceeded by calculating the initial $CO_2$ concentration of and $CO_2$ final concentration

by using Equation 4-5 to obtain the result as given in Table 1.

**Table 1**. Adsorption results using the sv[3]ko method

| **Finding the Optimum Conditions (qe Max) of $CO_2$ Adsorption** | | | | |
|---|---|---|---|---|
| **RUN 1-9** | | | | |
| **Fixed variables** | m, C0, T, t, P1 | | | |
| **Independent variable** | U | C | | |
| | | C1:8 % | C2:9 % | C3:10 % |
| **qe (%vol) (efficiency / capacity)** | U1:50 | *31.14 / 77.59* | *18.92 / 47.15* | *16.64 /41.45* |
| | U2:100 | *21.10 /52.56* | *19.62 /48.89* | *25.52 / 63.57* |
| | U3:150 | *29.01 /72.27* | *33.01 /82.22* | *32.77 /81.64* |
| **Eliminated Variables** | C1, U1, C2, U1, C3, U1, C1, U2, C2, U2, C3, U2, C1, U3, C3, U3 | | | |
| **Selected variables** | m, C0, T, t, P1, C2, U3 | | | |
| **RUN 10-17** | | | | |
| **Fixed variables** | m, C0, T, t, C2, U3 | | | |
| **Independent variable** | t | P | | |
| | | P1:2 Bar | P2:3 Bar | P3:4 Bar |
| **qe (%vol) (efficiency /performance)** | t1:30 | *33.01 / 82.22* | *31.04 / 92.42* | *8.08/ 24.87* |
| | t2:60 | *17,68 / 44,06* | *28,44 / 84.69* | *10.49 / 32.23* |
| | t3:120 | *11.59 / 28.89* | *22.2/ 66.23* | *12.21 / 37.55* |
| **Unselected variables** | T1, P2, T1, P3, T2, P1, T2, P2, T2, P3, T3, P1, T3, P2, T3, P3 | | | |
| **if qe not 1 > qe *max* 2 Selected variable (optimum condition)** | m, C0, t1, P1, C1, U1 | | | |
| **if qe not 1 < qe *max* 2 Selected variable (optimum condition)** | m, C0, t3, P3, C1, U1 | | | |

### 3.2.1. Effect Acid Concentration and Particle Size on the Adsorption Performance

Given by Figure 6, at mesh 50, the highest $CO_2$ adsorption efficiency was recorded at 31.148% vol at 8% HCl concentration but decreased drastically to 18.929% vol and 16.641% vol when the HCl concentration was increased to 9% and 10% (Liu et al., 2020). At mesh 100, the efficiency slightly decreased at 9% HCl concentration compared to 8% but increased significantly at 10% HCl concentration to reach 25.524% vol (Sun et al., 2017). Meanwhile, at mesh 150, the highest efficiency was found at 9% HCl concentration with a value of 33.01% vol, indicating that this concentration provides an optimal balance between material dissolution and active site formation (Lacinska et al., 2016).

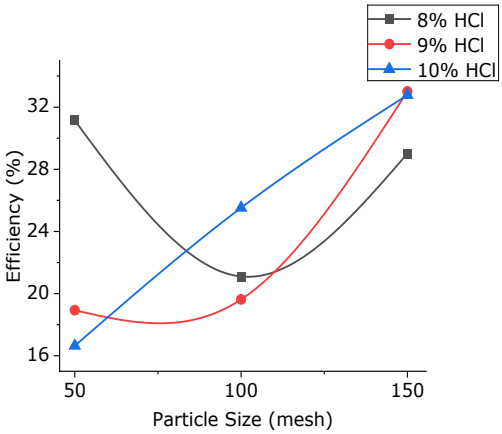


**Figure 6.** Adsorption Efficiency as the Function of Acid Concentration and Particle Size

In terms of $CO_2$ adsorption capacity, the results showed that at Figure 7 mesh 50, the adsorption capacity was relatively high at 8% HCl concentration but decreased as the HCl concentration increased. At mesh 100, the adsorption capacity increased as the HCl concentration increased, with the highest achievement at 10% HCl. For mesh 150, the highest adsorption capacity was also found at 9% HCl concentration with the amount of 0.0488 (gr adsorbent/gr $CO_2$), indicating that these conditions are optimal for forming stable and effective active sites.

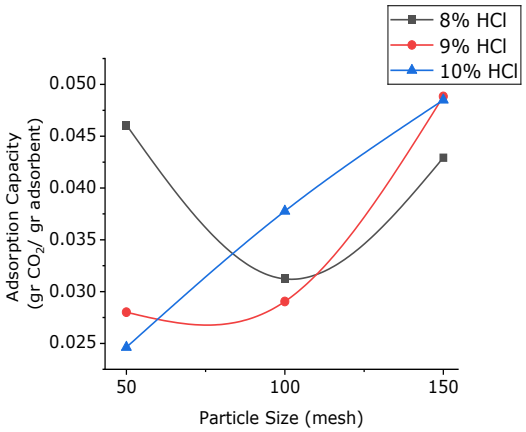


**Figure 7**. Adsorption Capacity as the Function of Acid Concentration and Particle Size

But in some cases, there is a potential for the error factor to consider. For example, like pressure, Li (2023) explain that pressure

enhances gas adsorption but also can lead to blockage and limited diffusion. Hazra (2018) also mentioned in his research that particle size plays the role of adsorption. On their study which explained by Li (2020), Chemical Activation also alter the chemical structure by enhancing the surface area and creating the active sites for $CO_2$ adsorption but excessive or in this case, prolonged activation process can lead to structural degradation for serpentine itself. Even the condition or the integrity of the reactor itself which also affects the efficiency of the adsorption.

### 3.2.2. Pressure and Time Effect on the Adsorption Performance

For the Pressure on Time test, the variable with the best results from the previous test was used, namely Mesh 150 activated with a concentration of 9% HCl using the $S_3VKO$ method where the best variable would be used, and the opposite would not be used which can be seen at Figure 8 and Figure 9 below. $CO_2$ adsorption using HCl-activated serpentine is effective for capturing CO2 gas. The activation enhances serpentine's adsorption capacity by substituting large cations with H+ ions, improving pore distribution (Hernández-Espinosa et al., 2018). At 2 bar pressure, adsorption efficiency starts at 33.01% after 30 minutes but drops to 11.60% after 120 minutes due to saturation (Kiełbasa et al., 2022). At 3 bar, efficiency decreases more gradually from 31.04% to 22.25% over the same period, suggesting that higher pressure slows saturation (Li et al., 2015). At 4 bar, efficiency rises from 8.08% to 12.22%, indicating that longer time is needed to achieve optimal conditions at elevated pressures, as supported by studies related to pore distribution and adsorption capacity (Konlechner and Kappacher, 2021).

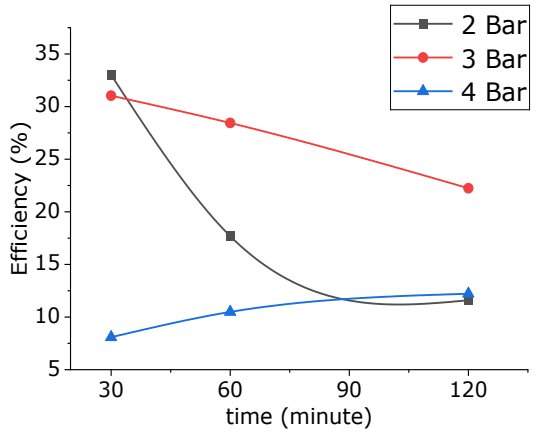


**Figure 8**. Adsorption Efficiency as the Function of Pressure and Time

This study evaluated the effect of time and pressure on $CO_2$ adsorption performance using HCl-activated serpentine. The results showed that at low pressure (2 bar), the $CO_2$ adsorption capacity was higher at the initial stage (0.488 g $CO_2$/g adsorbent in 30 min) compared to high pressure (4 bar, only 0.147 g $CO_2$/g adsorbent). This decrease in adsorption capacity is due to the rapid saturation of adsorption sites at high pressure (Srenscek-Nazzal et al., 2016). Over time, the adsorption capacity decreased, especially at low pressure, from 0.488 g $CO_2$/g adsorbent to 0.172 g $CO_2$/g adsorbent in 120 min (Abdullah, 2023). However, at 4 bar pressure, the adsorption capacity increased slightly from 0.147 g $CO_2$/g adsorbent to 0.223 g $CO_2$/g adsorbent over time, indicating that at low pressure, adsorption sites are more effectively utilized over time, with lower competition for active sites (Heidari et al., 2014).

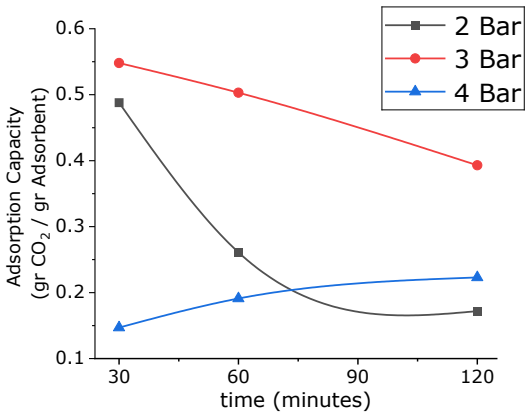


**Figure 9.** Adsorption Capacity as the Function of Pressure and Time

### 3.3. Adsorption Kinetic Model

### 3.3.1. Pseudo First Order

The first-order pseudo kinetics data showed that serpentine activated with 10% HCl gave the highest $CO_2$ absorption efficiency, with a coefficient of determination ($R^2$) of 0.979. The graph of the relationship between particle size (mesh) and ln(qe-qt) shows a straight line with a negative slope, resulting in the equation (y = -0.0068x + 0.3101). The high agreement between the experimental data and the equation of this line indicates that the first-order pseudo kinetic model is very suitable to describe the $CO_2$ adsorption process on serpentine activated with 10% HCl (Ho and McKay, 1999) shown by Figure 10.

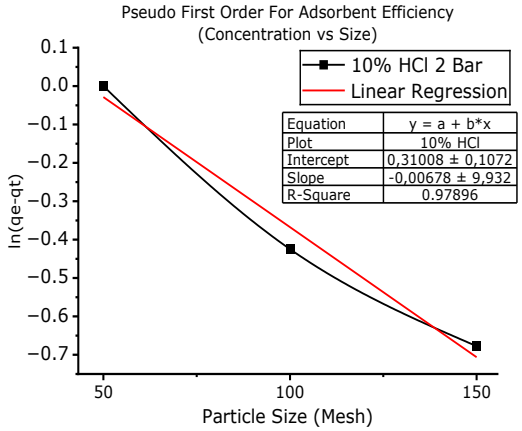


**Figure 10.** Adsorption Efficiency for the Pseudo First Order as the Function of Particle Size and Concentration

In this model, the graph is given by Figure 11, where the absorption rate is proportional to the number of active sites that have not yet been filled. The results of the analysis show that the linear equation generated from the plot ($\ln(q_e-q_t)$) against time is (y = -0.0068x + 0.309), with slope value ($k_1$) -0.0068 and intercept of 0.309. Coefficient of determination ($R^2$) obtained from this analysis is 0.978, which shows that the pseudo first order kinetics model is well suited to describe the $CO_2$ uptake data in activated serpentines (Ho and McKay, 1999).

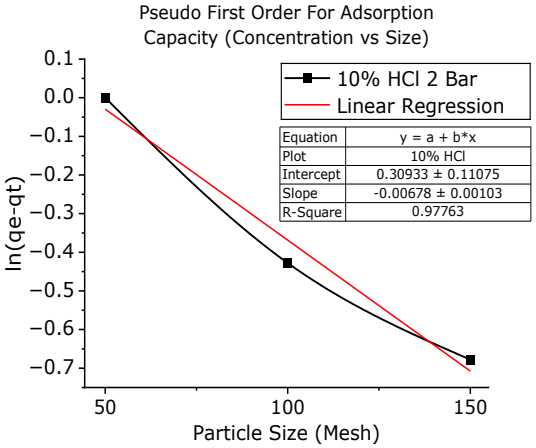


**Figure 11.** Adsorption Capacity for the Pseudo First Order as the Function of Particle Size and Concentration

As given by Figure 12, at a pressure of 4 bar, the efficiency of $CO_2$ absorption by serpentine increased with time. At 30 minutes, the efficiency was 00048 (g $CO_2$/g adsorbent). This figure continued to increase until it reached 0.00725 (g $CO_2$/g adsorbent) at 120 minutes. Analysis of the kinetics parameters revealed a rate constant ($k_1$) of 00038 min-¹. The coefficient of determination ($R^2$) of 0.9932 indicates the pseudo first order kinetic model is a good fit. This condition illustrates that the 4 bar pressure is the optimal condition to maximize the $CO_2$ absorption efficiency using serpentine adsorbent (Fatima et al., 2023).

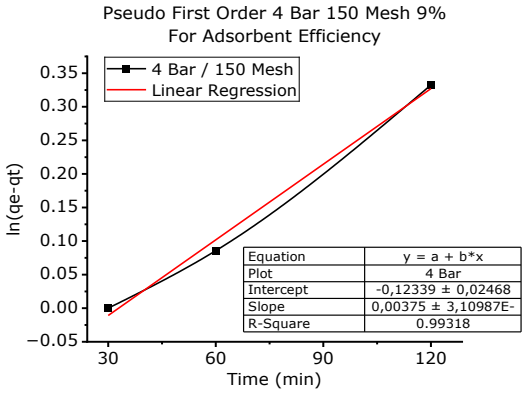


**Figure 12.** Adsorption Efficiency for the Pseudo First Order as the Function of Pressure and Time

Shown by Figure 13, at 3 bar where the adsorption rate constant tends to be higher which can indicate faster adsorption conditions with an $R^2$ value =0.9932 and this indicates that this model is accurate to represent the adsorption kinetics process. this shows that serpentine has a significant efficiency in adsorbing $CO_2$ for a pressure of 3 bar which makes it an ideal candidate for $CO_2$ absorption applications (Rashidi et al., 2021).

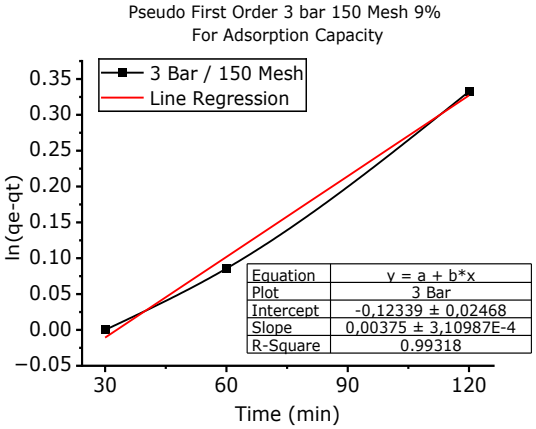


**Figure 13.** Adsorption Performance for the Pseudo First Order as the Function of Pressure and Time

### 3.3.2. Pseudo Second Order

The efficiency of $CO_2$ absorption by HCl-activated serpentines varies depending on the concentration of HCl used. The data showed at Figure 14, that $CO_2$ adsorption efficiency of HCl-activated serpentine depends on HCl concentration, with 10% HCl yielding the highest performance (qe = 0.067, R² =

0.9478), outperforming 9% (qe = 0.0287) and 8% HCl (qe = 0.8187, $R^2$ = 0.0208). The adsorption process follows a pseudo-second-order kinetics model, indicating faster and more efficient adsorption due to strong physical and chemical interactions on heterogeneous surfaces.(Ho and McKay, 1999).

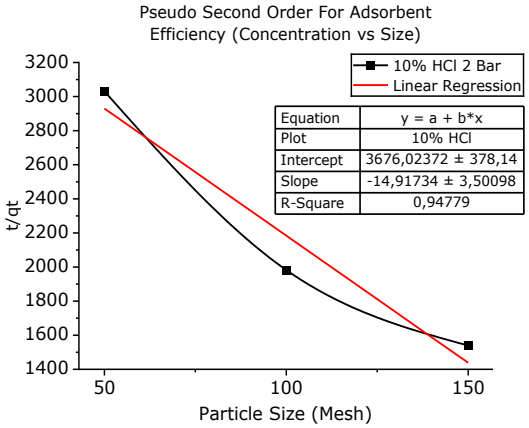


**Figure 14.** Adsorption Efficiency for the Pseudo Second Order as the Function of Size and Concentration

Plotted data on Figure 15, Serpentine activated with 10% HCl showed an adsorption capacity (qe) of 0.1667 mmol/g and a pseudo second order ($k_2$) rate constant of 0.0244 g/mmol·min. A correlation value ($R^2$) of 0.946 indicates that this model is well suited to describe adsorption kinetics under these conditions. Increased of $k_2$ compared to lower HCl concentrations indicates a faster rate of $CO_2$ adsorption on the serpentine surface, likely due to the increased number of active sites after activation with high concentrations of HCl (Tran, 2023).

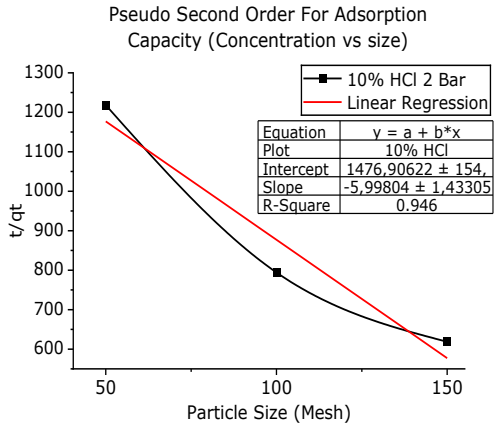


**Figure 15.** Adsorption Capacity for the Pseudo Second Order as the Function for Size and Concentration

For adsorption efficiency, the data shows on Figure 16 At 4 bar pressure, $CO_2$ adsorption efficiency by serpentine is maximized, with $R^2$ reaching a perfect value of 1 and a rate constant ($k_2$) of 4.6908. This indicates that the pseudo-second-order model accurately describes the adsorption process. Similar results were observed in Hafeez et al. (2015), where $R^2$ was also close to 1 under the same pressure conditions. Hafeez et al. (2015),

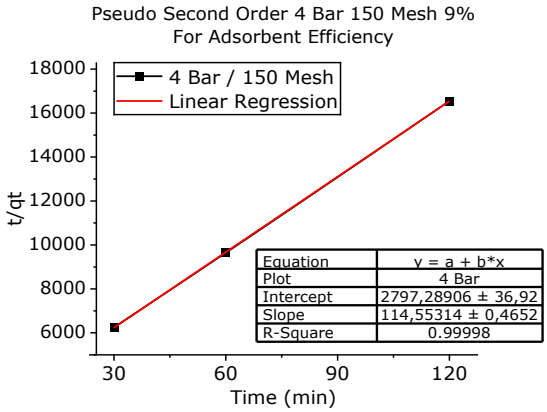


**Figure 16**. Adsorption Efficiency for the Pseudo Second Order as the Function of Time and Pressure

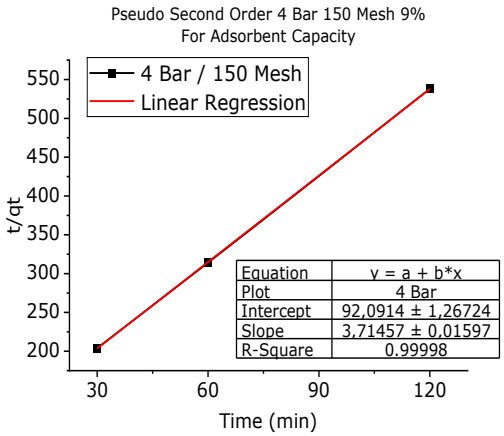


**Figure 17.** Graph of the Adsorption Performance for the Pseudo Second Order as the Function of Time and Pressure

The analysis of pseudo second order kinetics for $CO_2$ sorption given by Figure 17 using serpentine revealed that the optimal adsorption pressure is 4 bar, with a coefficient of determination $R^2$ of 1, indicating a perfect fit with the kinetic model. At this pressure, the adsorption rate constant $k_2$ is 0.1498, demonstrating high sorption efficiency for serpentine. This finding aligns with literature suggesting that pseudo second order models typically provide a better fit than pseudo first order models in $CO_2$ sorption processes, particularly for adsorbents like serpentine and activated carbon, which possess significant

active sites for adsorption. (Rashidi et al., 2021; Shikuku and Mishra, 2021).

### 3.4. Adsorption Isotherm Model

#### 3.4.1. Langmuir Isotherm

In this study, Figure 18 demonstrates the application of the Langmuir isotherm model to $CO_2$ adsorption on serpentine at a 150-mesh particle size, yielding an $R^2$ value of 0.9999, which supports strong monolayer adsorption on a homogeneous surface. The adsorption capacity ($q_m$) was recorded as -0.9686 (% vol), with a Langmuir constant $K_L$ of -24.581, indicating moderate affinity, and an adsorption energy (ΔE) of -7937.11 J/mol, suggesting a stable, exothermic process. These findings align with other studies showing that negative adsorption energy and Gibbs free energy imply a spontaneous and stable adsorption process. Similar studies by Du (2021) and (Ammendola et al., 2017) found negative Gibbs free energy and enthalpy values in $CO_2$ adsorption on high-rank coals and activated carbon, indicating spontaneous adsorption. Li (2020) and Song (2017) also reported negative Gibbs energy for $CO_2$ adsorption on similar materials, supporting the applicability of the Langmuir model in this analysis.

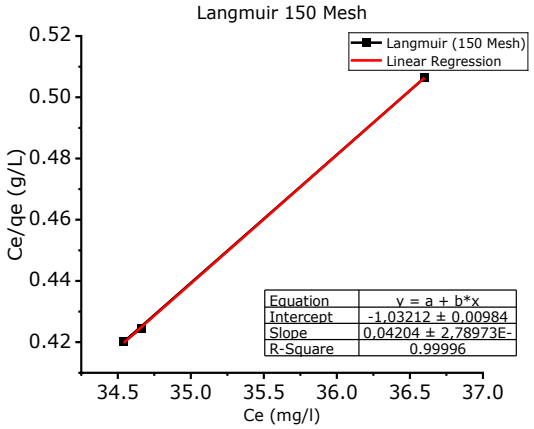


**Figure 18.** Langmuir Curve on 150 Mesh

Graph shown on Figure 19 shows that a 30-minute contact time achieved the highest $R^2$ value of 0.7573, indicating near-equilibrium adsorption within this period. This finding is consistent with Esmaeili (2019), who observed that shorter contact times optimize $CO_2$ adsorption by reaching rapid adsorption before saturation effects. The adsorption energy (ΔE) at 30 minutes is -8545.09 J/mol, signifying strong initial interactions, as also noted by Tiwari (2018), who found higher early-stage adsorption energies favouring quick $CO_2$ binding. The Langmuir constant ($K_L$) of -31.4137 reflects significant affinity during this initial phase, aligning with Goel (2017), who highlighted that high affinity in short-duration processes enhances $CO_2$ capture efficiency before equilibrium or desorption can impact adsorption.

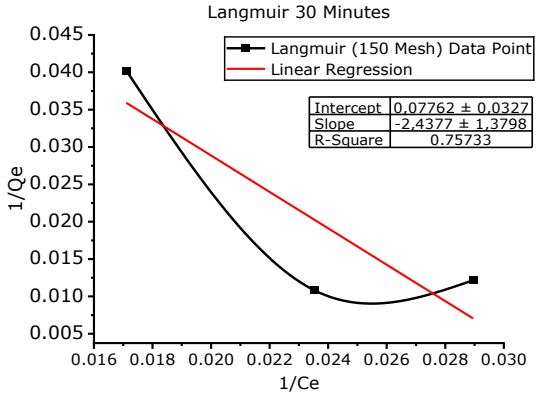


**Figure 19.** Langmuir Curve on 30 minutes

#### 3.4.2. Freundlich Isotherm

In the isotherm analysis of $CO_2$ absorption using HCl-activated serpentine which graph is given by Figure 20, the best results were obtained at a mesh size of 150. This is indicated by the value of $R^2$ = 1, which indicates the perfect match between Freundlich's isotherm model and the experimental data.

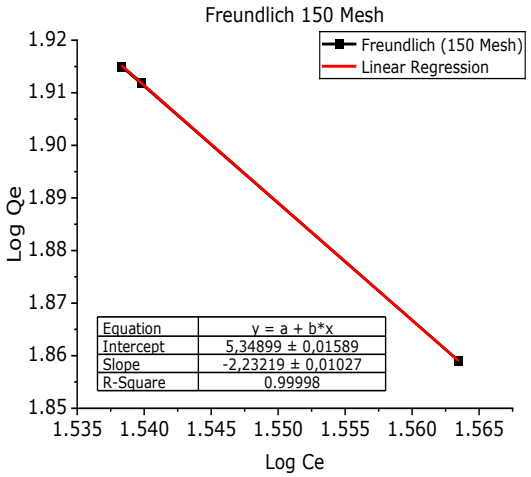


**Figure 20.** Freundlich Curve on 150 Mesh

Chemical activation with HCl results in significant changes in the surface structure of the serpentine, which increases the surface area and number of active sites available for adsorption, resulting in higher adsorption efficiency (Khalili et al., 2015). Freundlich's model is more suitable for describing experimental data at a mesh size of 150, with

a value of 1/nf = -2.2322 which indicates that the serpentine surface has a heterogeneous energy distribution, according to the characteristics of the chemically activated material (Soni et al., 2021).

Curve from Figure 21 illustrates the Freundlich isotherm model for $CO_2$ adsorption on serpentine at a 30-minute contact time, yielding an $R^2$ value of 0.7849 as the highest among tested times—indicating a reasonable fit for multilayer adsorption. The Freundlich constant $K_f$ = 567,022.12 L/mg reflects a high adsorption capacity, supporting serpentine's heterogeneous surface for multilayer adsorption. This aligns with Raganati (2018), who found that the Freundlich model effectively captured $CO_2$ adsorption on heterogeneous materials like carbon-magnetite composites. The heterogeneity factor $n_f$ = -0.4117 further indicates substantial surface heterogeneity, consistent with findings by Li and Hitch (2016), who demonstrated that serpentine-based materials support diverse adsorption sites, accommodating multilayer adsorption effectively.

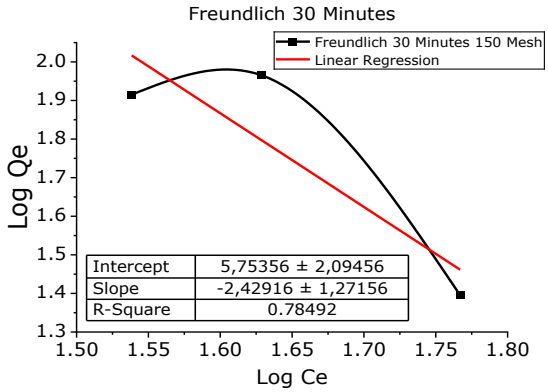


**Figure 21.** Freundlich Curve on 30 Minutes

## 4. Conclusion

In this study, $CO_2$ adsorption on 9% HCl-activated serpentine was optimized, with the 150-mesh particle size delivering the best results: an adsorption efficiency of 33.01% vol and an adsorption capacity of 82.29%. Under 2 bar pressure for 30 minutes, the concentration of adsorbed $CO_2$ reached 35.54% vol. In terms of adsorption kinetics, the Pseudo-Second Order (PSO) model proved superior to the Pseudo-First Order (PFO) model, indicating chemisorption as the main mechanism. For concentration vs. particle size (U vs. C) analysis at 10% HCl concentration, the PSO model showed high $R^2$ values (0.979 for efficiency and 0.9776 for performance), highlighting 10% HCl as optimal for effective surface activation. For pressure vs. time (P vs. T) analysis, the PSO model achieved the best fit at 4 bar pressure with $R^2$ = 1.0 for both efficiency and performance, suggesting that 4 bar optimally enhances the adsorption rate and capacity on serpentine. The isotherm analysis provided further insights into the adsorption mechanisms. For 150 mesh, both Langmuir and Freundlich models exhibited ideal fits, with $R^2$ = 0.9999 for Langmuir (supporting monolayer adsorption with adsorption energy, ΔE = -7937.11 J/mol) and $R^2$ = 1.0 for Freundlich (indicating multilayer adsorption with a $K_f$ of 223,357.22 L/mg on heterogeneous sites). Regarding contact time, the Freundlich model performed best at 30 minutes ($R^2$ = 0.7849, $K_f$ = 567,022.12 L/mg), suggesting effective multilayer adsorption within this short period. Future research should explore alternative activators, such as $HNO_3$ and $H_2SO_4$, investigate temperature effects, and develop serpentine-based nanomaterials to further improve adsorption capacity. Scaling up experiments and testing under real-world conditions (e.g., fluctuating pressures and temperatures) will be crucial to assess serpentine's feasibility for industrial-scale $CO_2$ capture. This study establishes HCl-activated serpentine as a promising adsorbent with significant potential for scalable carbon capture applications.

## Author contribution statement

Project Idea, H., A.A.R; Conceptualization, Writing–Original Draft, Editing Investigation, Analysis, M.F.D.; Supervision, Writing, Editing, M., N.R; Funding, Advisor H.H; Administration, D.D; Equipment Repair, F.

## Data availability statement

The data presented in this work/study are available.

## Declaration of Competing Interest

The authors declare no conflict of interest, The authors declare that they have no competing interests.

## Acknowledgements

This research and it's working is supported by Syiah Kuala University, Ministry of Education, Culture, Research, and Technology in accordance with the Letter of Assignment for the Implementation of Professor Research for the 2024 Fiscal Year Number: 106/UN11.2.1/PG.01.03/SPK/PTNBH/2024 dated May 3, 2024.

## References

Abdullah, M.F., (2023) Physicochemical and adsorption properties of guava leaves-activated carbon by hydrochloric acid on adsorption of methylene blue, *Scientific Research Journal,* 20, 33–49. https://doi.org/10.24191/srj.v20i1.20669

Ammendola, P., Raganati, F., Chirone, R., (2017) CO2 adsorption on a fine activated carbon in a sound assisted fluidized bed: Thermodynamics and kinetics, *Chemical Engineering Journa,l* 322, 302–313. https://doi.org/10.1016/j.cej.2017.04.037

Ardiansyah, E.Y., Syafriadi, S., Tibri, T., Eka Onwardana, M., Sungen, S., (2019) POTENSI SERPENTINIT UNTUK PEMANFAATAN BAHAN BAKU PUPUK MINERAL, *Saintek ITM*, 32. https://doi.org/10.37369/si.v32i1.53

Beglaryan, H., Isahakyan, A., Zulumyan, N., Melikyan, S., Terzyan, A., (2023) A study of magnesium dissolution from serpentinites composed of different serpentine group minerals, *Minerals Engineering,* 201, 108171. https://doi.org/10.1016/j.mineng.2023.108171

Burke, A., Fishel, S., (2020) A coal elimination treaty 2030: Fast tracking climate change mitigation, global health and security, *Earth System Governance,* 3, 100046. https://doi.org/10.1016/j.esg.2020.100046

Daval, D., Hellmann, R., Martinez, I., Gangloff, S., Guyot, F., (2013) Lizardite serpentine dissolution kinetics as a function of pH and temperature, including effects of elevated pCO2, *Chemical Geology,* 351, 245–256. https://doi.org/10.1016/j.chemgeo.2013.05.020

Du, X., Cheng, Y., Liu, Z., Yin, H., Wu, T., Huo, L., Shu, C., (2021) CO2 and CH4 adsorption on different rank coals: A thermodynamics study of surface potential, Gibbs free energy change and entropy loss, *Fuel,* 283, 118886. https://doi.org/10.1016/j.fuel.2020.118886

Esmaeili, F., Gholami, M., Hojjat, M., (2019) Accelerated CO2 capture on adsorbent coated finned tube: An experimental study, *Energy,* 187, 116014. https://doi.org/10.1016/j.energy.2019.116014

Falini, G., Foresti, E., Gazzano, M., Gualtieri, A.E., Leoni, M., Lesci, I.G., Roveri, N., (2004) Tubular-shaped stoichiometric chrysotile nanocrystals, *Chemistry - A European Journal,* 10, 3043–3049. https://doi.org/10.1002/chem.200305685

Fatima, S.S., Borhan, A., Ayoub, M., Ghani, N.A., (2023) Modeling of CO2 Adsorption on Surface-Functionalized Rubber-Seed Shell Activated Carbon: Isotherm and Kinetic Analysis, *Processes,* 11. https://doi.org/10.3390/pr11102833

Goel, C., Tiwari, D., Bhunia, H., Bajpai, P.K., (2017) Pure and Binary Gas Adsorption Equilibrium for CO2-N2 on Oxygen Enriched Nanostructured Carbon Adsorbents, *Energy and Fuels,* 31, 13991–13998. https://doi.org/10.1021/acs.energyfuels.7b02671

Hafeez, S., Fan, X., Hussain, A., Martín, C.F., (2015) CO2 adsorption using TiO2 composite polymeric membranes: A kinetic study, *Journal of Environmental Sciences (China),* 35, 163–171. https://doi.org/10.1016/j.jes.2015.04.019

Hazra, B., Wood, D.A., Vishal, V., Singh, A.K., (2018) Pore Characteristics of Distinct Thermally Mature Shales: Influence of Particle Size on Low-Pressure CO2 and N2 Adsorption, *Energy and Fuels*, https://doi.org/10.1021/acs.energyfuels.8b01439

Heidari, A., Younesi, H., Rashidi, A., Ghoreyshi, A.A., (2014) Evaluation of CO2 adsorption with eucalyptus wood based activated carbon modified by ammonia solution through heat treatment, *Chemical Engineering Journal*, 254, 503–513. https://doi.org/10.1016/j.cej.2014.06.004

Hernández-Espinosa, M.A., Quiroz-Estrada, K., Petranovskii, V., Rojas, F., Portillo, R., Salgado, M.A., Marcelo, M., Rubio, E., Felipe, C., (2018) Adsorption of N2, No2 and $CO_2$ on epistilbite natural zeolite from Jalisco, Mexico after acid treatment, *Minerals,* 8.

https://doi.org/10.3390/min8050196

Ho, Y.., McKay, G., (1999) Pseudo-second order model for sorption processe, *Process Biochemistry,* 34, 451–465. https://doi.org/10.1016/S0032-9592(98)00112-5

Khalili, S., Khoshandam, B., Jahanshahi, M., (2015) Optimization of production conditions for synthesis of chemically activated carbon produced from pine cone using response surface methodology for CO2 adsorption, *RSC Advances,* 5, 94115–94129. https://doi.org/10.1039/c5ra18986a

Kiełbasa, K., Bayar, Ş., Varol, E.A., Sreńscek-Nazzal, J., Bosacka, M., Miądlicki, P., Serafin, J., Wróbel, R.J., Michalkiewicz, B., (2022) Carbon Dioxide Adsorption over Activated Carbons Produced from Molasses Using H2SO4, H3PO4, HCl, NaOH, and KOH as Activating Agents, *Molecules,* 27. https://doi.org/10.3390/molecules27217467

Kim, K.H., Kim, M.H., (2023) Adsorption of CO2, CO, H2, and N2 on Zeolites, Activated Carbons, and Metal-Organic Frameworks with Different Surface Nonuniformities, *Sustainability,* 15, 11574. https://doi.org/10.3390/su151511574

Konlechner, D., Kappacher, G., (2021) Achieving the Carbon-Neutral Production of Magnesia and Silica Products Using a HCl-Based Process in Serpentine *Feedstock,* 19. https://doi.org/10.3390/materproc2021005019

Lacinska, A.M., Styles, M.T., Bateman, K., Wagner, D., Hall, M.R., Gowing, C., Brown, P.D., (2016) Acid-dissolution of antigorite, chrysotile and lizardite for ex situ carbon capture and storage by mineralisation, *Chemical Geology,* 437, 153–169. https://doi.org/10.1016/j.chemgeo.2016.05.015

Li, J., Hitch, M., (2016) Carbon dioxide adsorption isotherm study on mine waste for integrated CO2 capture and sequestration processes, *Powder Technology,* 291, 408–413. https://doi.org/10.1016/j.powtec.2015.12.011

Li, J., Hitch, M., (2015) Carbon dioxide sorption isotherm study on pristine and acid-treated olivine and its application in the vacuum swing adsorption process, *Minerals,* 5, 259–275. https://doi.org/10.3390/min5020259

Li, J., Yang, Y., Wen, Y., Liu, W., Chu, Y., Wang, R., Xu, Z., (2020) Leaching kinetics and mechanism of laterite with NH4 Cl-HCl solution, *Minerals,* 10, 1–11. https://doi.org/10.3390/min10090754

Li, L., Si, J., Li, Z., Cheng, G., Chen, J., (2023) Experimental Study on Influencing Factors and Thermal Effects of CO2 Adsorption by Coal, *ACS Omega,* 8, 21906–21913. https://doi.org/10.1021/acsomega.3c01693

Li, S., Deng, S., Zhao, L., Yuan, X., Yun, H., (2020) How to express the adsorbed CO2 with the Gibbs' thermodynamic graphical method: A preliminary study, *Energy*, 193, 116753. https://doi.org/10.1016/j.energy.2019.116753

Li, Y., Wang, W., Cheng, X., Su, M., Ma, X., Xie, X., (2015) Simultaneous CO2/HCl removal using carbide slag in repetitive adsorption/desorption cycles, *Fuel,* 142, 21–27. https://doi.org/10.1016/j.fuel.2014.10.071

Lin, P.C., Huang, C.W., Hsiao, C.T., Teng, H., (2008) Magnesium hydroxide extracted from a magnesium-rich mineral for CO 2 sequestration in a gas-solid system, *Environmental Science and Technology,* 42, 2748–2752. https://doi.org/10.1021/es072099g

Liu, B., Guo, W., Wang, H., Si, Q., Zhao, Q., Luo, H., Ren, N., (2020) B-doped graphitic porous biochar with enhanced surface affinity and electron transfer for efficient peroxydisulfate activation, *Chemical Engineering Journal,* 396, 125119. https://doi.org/10.1016/j.cej.2020.125119

Muslim, A., Purnawan, E., Nasrullah, Meilina, H., Azwar, M.Y., Deri, N.O., Kadri, A., (2022) Adsorption of Copper Ions Onto Rice Husk Activated Carbon Prepared Using Ultrasound Assistance: Optimization Based on Step-By-Step Single Variable Knockout Technique,

*Journal of Engineering Science and Technology,* 17, 2496–2511.

Raganati, F., Alfe, M., Gargiulo, V., Chirone, R., Ammendola, P., (2018) Isotherms and thermodynamics of CO2 adsorption on a novel carbon-magnetite composite sorbent, *Chemical Engineering Research and Design,* 134, 540–552. https://doi.org/10.1016/j.cherd.2018.04.037

Rashidi, N.A., Bokhari, A., Yusup, S., (2021) Evaluation of kinetics and mechanism properties of CO2 adsorption onto the palm kernel shell activated carbon, *Environmental Science and Pollution Research,* 28, 33967–33979. https://doi.org/10.1007/s11356-020-08823-z

Russel, Cl., (2023) Asia's coal sector sees long, prosperous life [WWW Document]. URL https://www.nst.com.my/opinion/columnists/2023/09/961251/asias-coal-sector-sees-long-prosperous-life (accessed 12.6.23).

Sanna, A., Steel, L., Maroto-Valer, M.M., (2017) Carbon dioxide sequestration using NaHSO 4 and NaOH: A dissolution and carbonation optimisation study, *Journal of Environmental Management,* 189, 84–97. https://doi.org/10.1016/j.jenvman.2016.12.029

Shikuku, V.O., Mishra, T., (2021) Adsorption isotherm modeling for methylene blue removal onto magnetic kaolinite clay: a comparison of two-parameter isotherms, *Applied Water Science,* 11, 1–9. https://doi.org/10.1007/s13201-021-01440-2

Song, X., Wang, L., Ma, X., Zeng, Y., (2017) Adsorption equilibrium and thermodynamics of CO 2 and CH 4 on carbon molecular sieves, *Applied Surface Science,* 396, 870–878. https://doi.org/10.1016/j.apsusc.2016.11.050

Soni, P., Sur, A., Gaba, V.K., Sah, R.P., (2021) Review on improvement of adsorption refrigeration systems performance using composite adsorbent: current state of art, *Energy Sources, Part A: Recovery, Utilization and Environmental Effects,* 00, 1–25. https://doi.org/10.1080/15567036.2021.1927252

Srenscek-Nazzal, J., Narkiewicz, U., Morawski, A.W., Wróbel, R.J., Michalkiewicz, B., (2016) The Increase of the Micoporosity and CO2 Adsorption Capacity of the Commercial Activated Carbon CWZ-22 by KOH Treatment, in: Microporous and Mesoporous Materials, *InTech*, p. 15. https://doi.org/10.5772/63672

Sun, Y., Zhao, J., Wang, J., Tang, N., Zhao, R., Zhang, D., Guan, T., Li, K., (2017) Sulfur-Doped Millimeter-Sized Microporous Activated Carbon Spheres Derived from Sulfonated Poly(styrene-divinylbenzene) for CO2 Capture, *Journal of Physical Chemistry,* C 121, 10000–10009. https://doi.org/10.1021/acs.jpcc.7b02195

Tiwari, D., Bhunia, H., Bajpai, P.K., (2018) Adsorption and thermodynamic studies of pure and binary CO2 and N2 gas components on nitrogen enriched nanostructured carbon adsorbents, *Journal of Chemical Thermodynamics,* 125, 205–213. https://doi.org/10.1016/j.jct.2018.06.009

Tran, H.N., (2023) Applying Linear Forms of Pseudo-Second-Order Kinetic Model for Feasibly Identifying Errors in the Initial Periods of Time-Dependent Adsorption Datasets, *Water (Switzerland),* 15. https://doi.org/10.3390/w15061231

Vieira, K.R.M., Arce, G.L.A.F., Luna, C.M.R., Facio, V.O., Carvalho, J.A., Neto, T.G.S., Ávila, I., (2022a) Understanding the acid dissolution of Serpentinites (Tailings and waste rock) for use in indirect mineral carbonation, *South African Journal of Chemical Engineering,* 40, 154–164. https://doi.org/10.1016/j.sajce.2022.02.005

Vieira, K.R.M., Arce, G.L.A.F., Luna, C.M.R., Facio, V.O., Carvalho, J.A., Neto, T.G.S., Ávila, I., (2022b) Understanding the acid dissolution of Serpentinites (Tailings and waste rock) for use in indirect mineral carbonation, *South African Journal of Chemical Engineering,* 40, 154–164. https://doi.org/10.1016/j.sajce.2022.02.005